

LETTER • OPEN ACCESS

# Nonlinear impacts of future anthropogenic aerosol emissions on Arctic warming

To cite this article: S Dobricic *et al* 2019 *Environ. Res. Lett.* **14** 034009

View the [article online](#) for updates and enhancements.

## Environmental Research Letters



## LETTER

## Nonlinear impacts of future anthropogenic aerosol emissions on Arctic warming

## OPEN ACCESS

## RECEIVED

26 November 2018

## ACCEPTED FOR PUBLICATION

17 December 2018

## PUBLISHED

13 March 2019

Original content from this work may be used under the terms of the [Creative Commons Attribution 3.0 licence](#).

Any further distribution of this work must maintain attribution to the author(s) and the title of the work, journal citation and DOI.

S Dobricic<sup>1</sup> , L Pozzoli<sup>1</sup>, E Vignati<sup>1</sup>, R Van Dingenen<sup>1</sup>, J Wilson<sup>1</sup>, S Russo<sup>1</sup> and Z Klimont<sup>2</sup><sup>1</sup> European Commission, Joint Research Centre, Ispra, Italy<sup>2</sup> International Institute for Applied Systems Analysis, Laxenburg, AustriaE-mail: [srdan.dobricic@ec.europa.eu](mailto:srdan.dobricic@ec.europa.eu)**Keywords:** Arctic warming, climate change, air pollutionSupplementary material for this article is available [online](#)**Abstract**

Past reductions of anthropogenic aerosol concentrations in Europe and North America could have amplified Arctic warming. In the future the impact of air pollution policies may differ, because the major anthropogenic sources of atmospheric aerosols are increasingly located in Asia. In this study numerical experiments evaluating only direct aerosol effects on atmospheric temperatures indicate that, while reduced carbon dioxide (CO<sub>2</sub>) emissions weaken Arctic warming, direct radiative forcing effects by reductions of anthropogenic aerosol concentrations, additional to those obtained by lower CO<sub>2</sub> emissions, can either amplify or diminish it. Interactions between regionally modified radiation in Asia and internal climate variability may differently initiate and sustain atmospheric planetary waves propagating into the Arctic. In a nonlinear manner planetary waves may redistribute atmospheric and oceanic meridional heat fluxes at the high latitudes and either amplify or diminish Arctic warming in 2050. Lower CO<sub>2</sub> concentrations might apparently contribute to reduce the interactions between the Arctic system and the lower latitudes, thus reducing the influence of strong air quality measures in Asia on the Arctic amplification of global warming. While past and present air pollution policies could have amplified Arctic warming, in the future the effects from atmospheric pollution reductions are less certain, depending on the future CO<sub>2</sub> concentrations, and requiring improved simulations of changing aerosol concentrations and their interactions with clouds in Asia and the Arctic.

**1. Introduction**

Currently the Arctic warms at a much higher rate than the rest of the globe. Its sea-ice cover is increasingly shrinking during summer and its volume does not fully recover in winter (Cohen *et al* 2014). The acceleration of warming may be due to natural climate variability (Swart *et al* 2015), deposition of black carbon (BC) on the sea and land ice (Clarke and Noone 1985, Hansen and Nazarenko 2004), albedo feedback over the ice-free ocean (Serreze and Francis 2006), global temperature feedbacks (Pithan and Mauritsen 2014), tropical forcing (Ding *et al* 2014), mid-latitude sea surface temperature forcing (Peings and Magnusdottir 2014, Perlwitz *et al* 2015) and anomalies in oceanographic transport into the Arctic (Årthun *et al* 2012).

The redistribution of anthropogenic aerosol emissions in the last decades in the Northern Hemisphere could have also significantly contributed to Arctic warming (Mitchell and Johns 1997, Yang *et al* 2014, Baker *et al* 2015, Najafi *et al* 2015, Stohl *et al* 2015, Acosta Navarro *et al* 2016). The reduction of sulphur dioxide (SO<sub>2</sub>) emissions in Europe since 1980 may have additionally increased the Arctic near-surface temperatures as much as 0.5 °C (Acosta Navarro *et al* 2016). The implementation of stringent air quality policies in Europe and North America together with the simultaneous growth of industrial production in South and East Asia has caused a shift in the magnitude and composition of pollutant emissions. SO<sub>2</sub> emissions doubled between 1990 and 2010 in China and India from about 20–40 Tg yr<sup>-1</sup>, and decreased by

70% in Europe and North America from about 52–16.5 Tg yr<sup>-1</sup> (Granier *et al* 2011, Smith *et al* 2011, Klimont *et al* 2013). Anthropogenic emissions of primary particulate matter with diameter below 2.5 μm dropped from 9–4 Tg yr<sup>-1</sup> in Europe and Russia, and from 2–1.3 in North America, while they increased in East Asia from 15–20 Tg year<sup>-1</sup>. Global BC emissions increased by 15% since 1990 despite strong reductions in Europe and North America (Klimont *et al* 2017).

The direct radiative forcing by aerosols in South and East Asia may interact with the monsoon activity and modify winds and precipitation (e.g. Li *et al* 2016, Jiang *et al* 2017). By diminishing the incoming radiation at the surface over land, increasing of both SO<sub>2</sub> and BC emissions may have reduced the monsoon precipitation in summer, partly offsetting the expected global warming effect due to higher global carbon dioxide (CO<sub>2</sub>) concentration (Mitchell and Johns 1997, Menon *et al* 2002, Ramanathan *et al* 2005, Bollasina *et al* 2011, Guo *et al* 2015). The effect of BC could be particularly intense due to the warming of lower troposphere by absorption of heat (Ramanathan *et al* 2005). Increasing aerosol concentrations over Asia force decadal variations of mid-latitude cyclones (Wang *et al* 2014) and intensify winds over the North Pacific Ocean (Takahashi and Watanabe 2016). Changes in natural aerosol concentrations in the tropics may initiate stationary planetary waves in the atmosphere (Lewinschal *et al* 2013) that propagate into the Arctic. This is consistent with modelling and observational findings on the remote impacts of heat anomalies in the tropical Pacific Ocean on the enhanced Arctic warming by the action of planetary waves (e.g. Ding *et al* 2014). Theoretically it can be expected that heat anomalies in Southeast Asia may force the atmospheric circulation in the high latitudes (e.g. Hoskins and Karoly 1981).

Historical pollution emission estimates contain regionally and temporally varying uncertainties, but generally they show a simultaneous reduction of pollution in Europe and North America and increase in Asia (e.g. Crippa *et al* 2016, Hoesly *et al* 2018, Klimont *et al* 2017). On the other hand, there is a larger uncertainty in estimating future pollution emissions (Amman *et al* 2013, Rao *et al* 2017). Although the geographical distribution of major sources of anthropogenic aerosol emissions has changed, even a future decrease in emissions in South and East Asia might accelerate the sea-ice melting in the Arctic (Westervelt *et al* 2015, Acosta Navarro *et al* 2017, Wang *et al* 2018). This means that likely more stringent air quality policies in the future require additional reductions in CO<sub>2</sub> concentrations in order to avoid the negative impact in the Arctic. Here we perform climate simulations until 2050 with an Earth system model that includes the coupling between the land, ocean, atmosphere and sea-ice. The study estimates how different aerosol reduction measures, considering consistent CO<sub>2</sub> emissions due to the burning of fossil and bio fuels

under two global warming scenarios, may impact Arctic temperatures and sea-ice melting through the propagation of regional radiative perturbations from the mid-latitudes associated to the direct aerosol forcing.

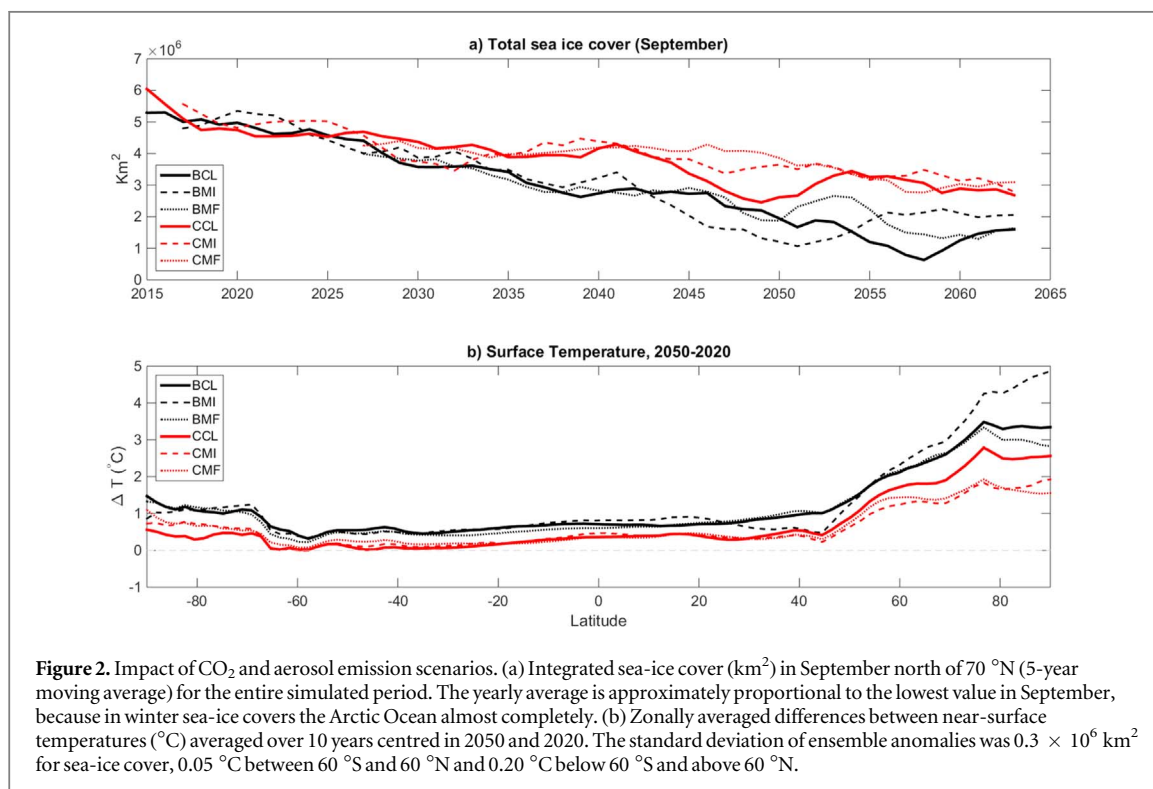
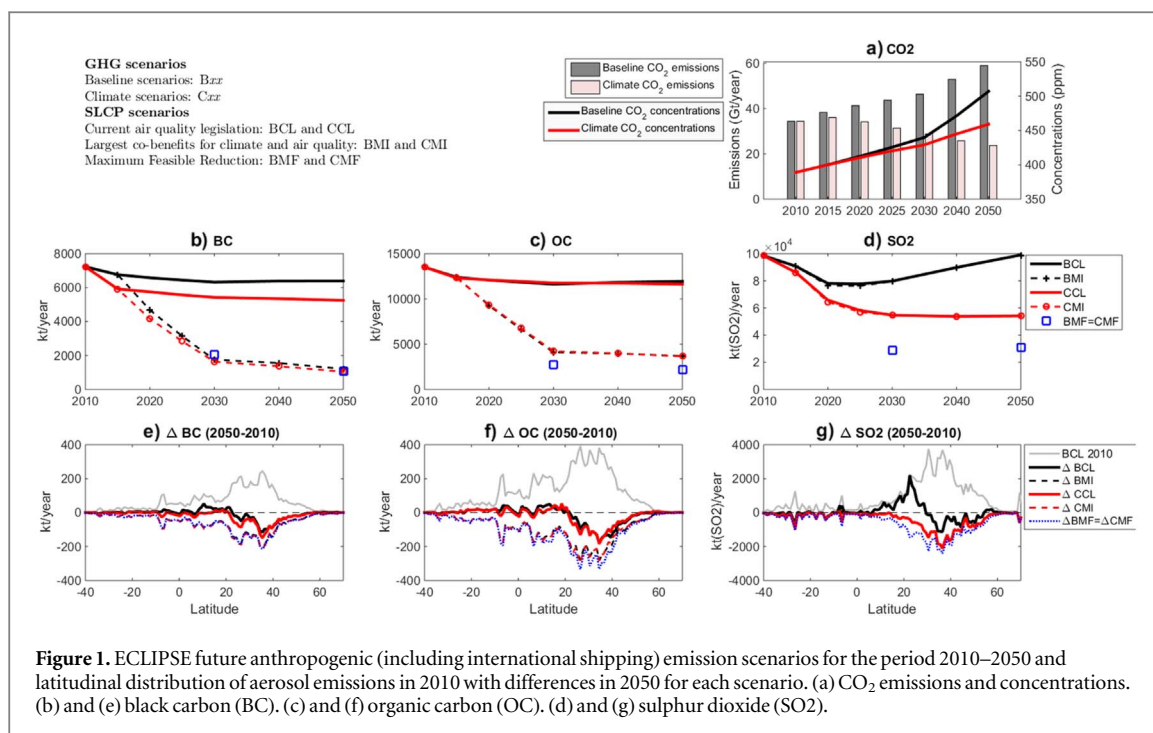
## 2. Methods

### 2.1. Earth system model

Simulations were performed by the fully coupled community earth system model (CESM) Version 1.2.2 (Hurrell *et al* 2013) developed at the National Centre for Atmospheric Research. CESM has been extensively evaluated and its performance has been compared with other climate models (e.g. Morgenstern *et al* 2017). The configuration contains the CAM4 atmospheric model (Neale *et al* 2010) with the MOZART4 chemistry (Emmons *et al* 2010) simulating the ozone photochemistry and aerosols (sulphate, nitrate, sea-salts, mineral dust, organic carbon, BC, and secondary organic aerosols), ocean model POP2 (Smith *et al* 2010), sea-ice model CICE (Hunke and Lipscomb 2008) and land model CLM4.0 (Oleson *et al* 2010). The horizontal resolution is 1.9° × 2.5° for the atmosphere with 26 hybrid sigma-pressure levels and 1° × 1° for the ocean and sea-ice with 60 levels in the ocean. The aerosol impact on the atmosphere is limited to the direct radiative forcing. The interaction between aerosols and cloud droplets, available in some other CESM configurations, is excluded considering a high uncertainty in simulating and estimating regional and global radiative impacts of these processes with coarse resolution climate models (e.g. Boucher *et al* 2013, Ma *et al* 2014), but findings are also evaluated in selected Coupled Model Intercomparison Project 5 (CMIP5) simulations containing indirect aerosol effects. The model includes deposited aerosols and melt ponds in the calculation of the scattering and absorption characteristics of ice and snow (Holland *et al* 2012).

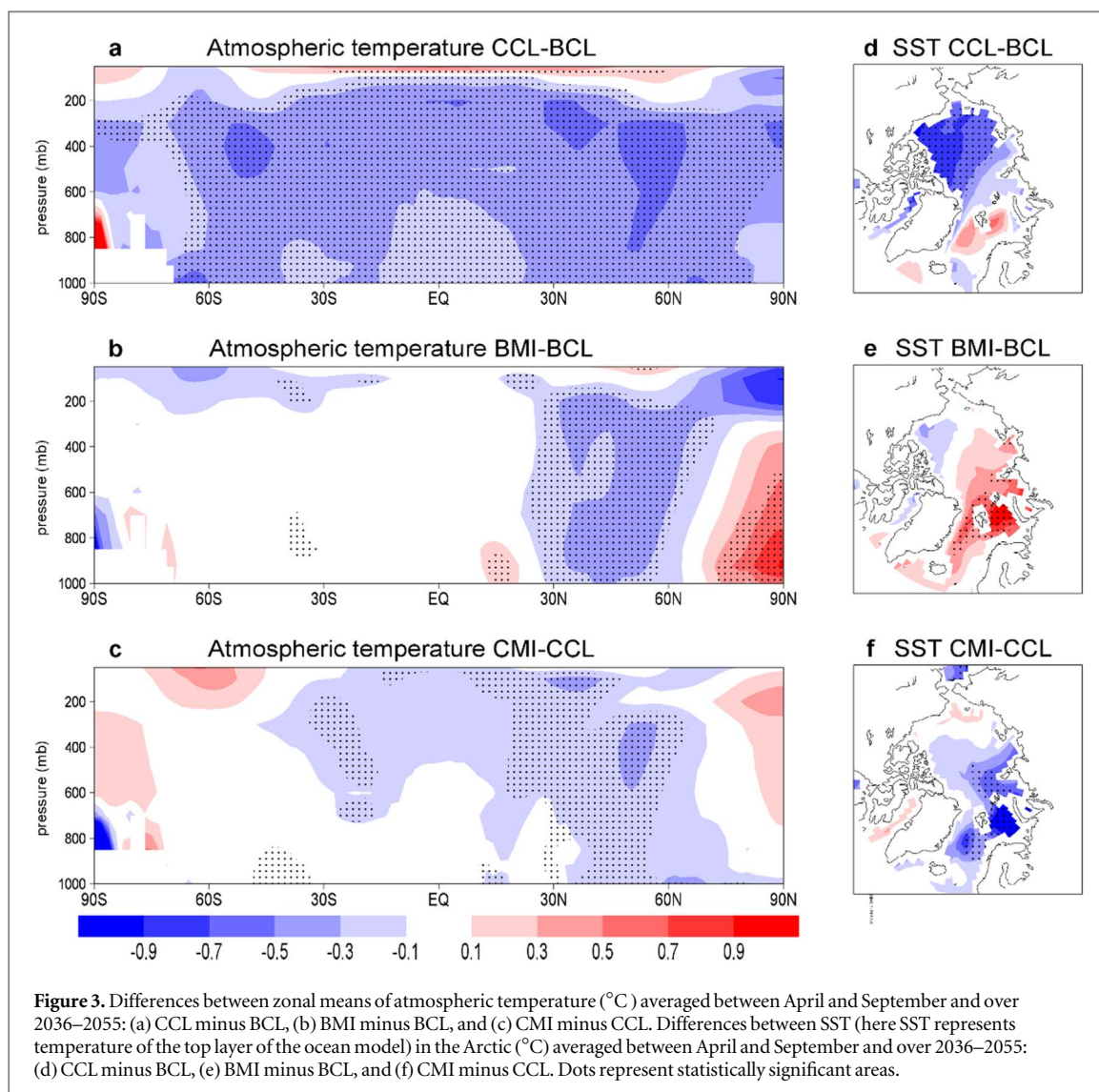
### 2.2. Experiments

Six experiments describe different scenarios of energy use, industrial production and agricultural activity until 2050 with consequent greenhouse gases (GHGs) concentration trajectories and different strategies to reduce the emissions of short lived climate pollutants (SLCP) (figure 1). There are two pathways of GHG concentrations mainly driven by the energy use defined in the International Energy Agency study (IEA 2012). The first, referred to as 'Baseline', is an extension of current trends with doubled energy use in 2050 compared to 2009 and absence of efforts to stabilize CO<sub>2</sub> atmospheric concentration. The second, named 'Climate', would give an 80% chance of keeping the mean global temperature increase below 2 °C by 2100 (figure 1(a)). Three mitigation scenarios reducing aerosol and ozone precursor emissions are combined with both the 'Baseline' and 'Climate'



GHG scenarios (figures 1(b)–(g), and supplementary figures S1 and S2 which are available online at [stacks.iop.org/ERL/14/034009/mmedia](https://stacks.iop.org/ERL/14/034009/mmedia)). The first assumes effective implementation of the air pollution current legislation such as the NEC directive for European Union or the China 12th Five-Year Plan (named BCL for Baseline and CCL for Climate scenario). The second introduces measures beyond current legislation which are characterized by the largest co-benefits for climate and air quality (named BMI for Baseline

and CMI for Climate scenario), based on the 20 years Global Temperature change Potential (GTP20) metric calculated for each SLCP emission type. These mitigation scenarios imply that sulphur emissions, potentially cooling the atmosphere through sulphate aerosol radiative forcing, are not affected when compared to the corresponding Baseline and Climate scenarios (figure 1(d)). The third assumes the maximum feasible reduction in air pollutants (named BMF for Baseline and CMF for Climate scenario).



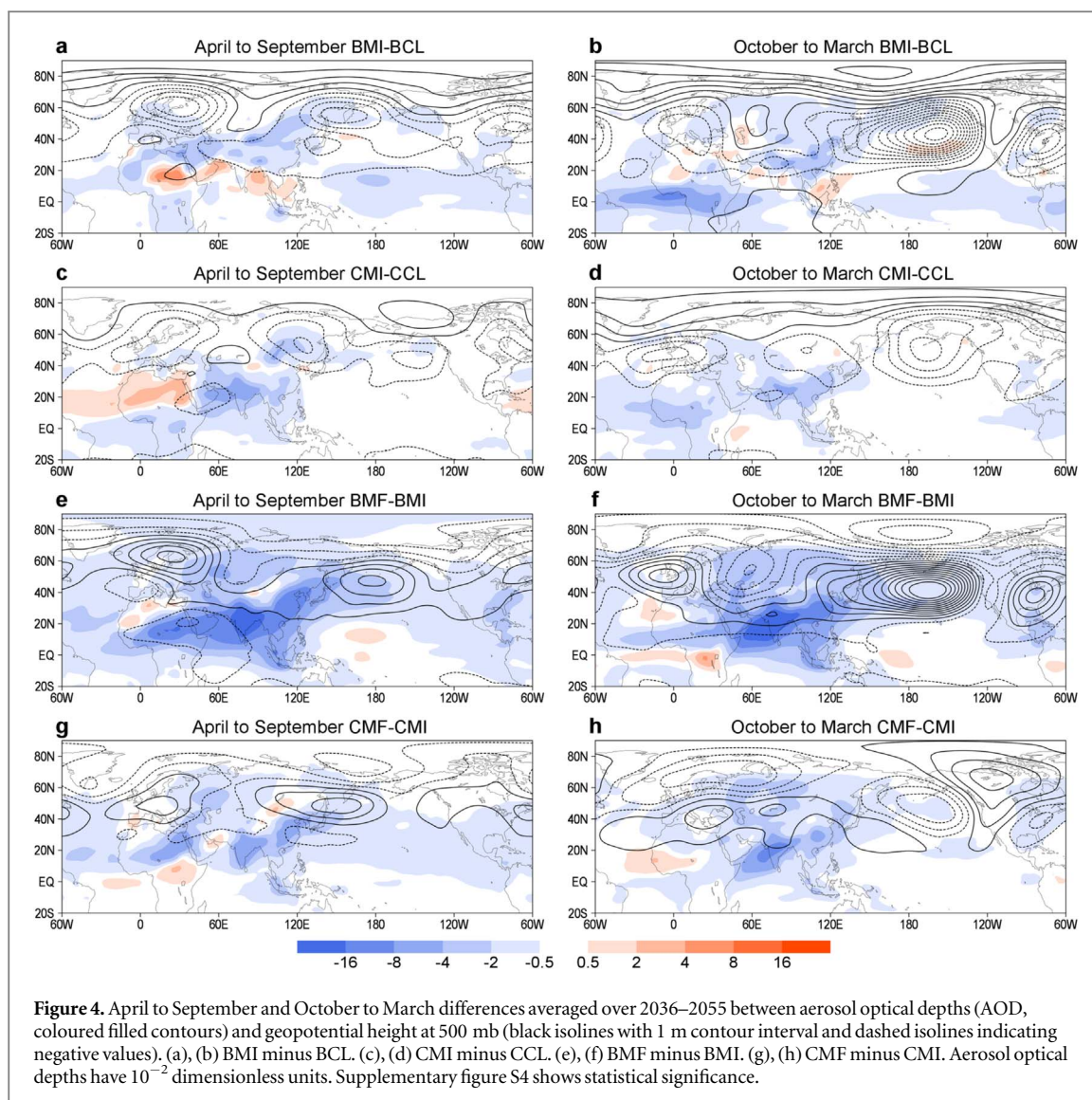
The six transient simulations make use of the ECLIPSEv5a anthropogenic emission scenarios of gases and aerosols (Stohl *et al* 2015) estimated from 2015–2050 (available at <http://www.iiasa.ac.at/web/home/research/researchPrograms/air/ECLIPSEv5a.html>) and further extended until 2065 with constant GHG concentrations and SLCP emissions of year 2050. Experiments are preceded by a 6 years long simulation starting from CESM initial conditions for year 2000 obtained in a climate simulation starting in 1850 from an equilibrium state.

In the ‘Baseline’ scenarios BCL and BMI global energy-related  $\text{CO}_2$  emissions increase by up to  $60 \text{ Gt yr}^{-1}$  reaching concentrations of more than 500 ppm in 2050 similar to the RCP6.0 scenario of IPCC AR5 (Lamarque *et al* 2010). The ‘Climate’ scenarios are based on the IEA  $2^{\circ}\text{C}$  energy scenario (IEA 2012), where  $\text{CO}_2$  emissions peak in 2015 and decrease to about  $24 \text{ Gt yr}^{-1}$  giving a concentration of about 450 ppm in 2050. In BMI and CMI ECLIPSEv5a includes reductions of SLCP targeting BC and ozone

mitigation similarly to the UNEP/WMO assessment (UNEP/WMO 2011, Shindell *et al* 2012).

Climate scenarios assume a large reduction of sulphur emissions co-occurring with reduced  $\text{CO}_2$  emissions resulting from declining use of fossil fuels and only minor changes in BC emissions. In BMI and CMI scenarios ECLIPSEv5a assumes additional measures for mitigating SLCP by further drastically reducing BC, organic carbon, as well several co-emitted species, including non-methane volatile organic compounds, carbon monoxide, and to some extent nitrogen oxides. With respect to BMI and CMI, the BMF and CMF scenarios from ECLIPSEv5a further assume a drastic reduction of  $\text{SO}_2$  emissions after 2030 and a modest reduction in OC emissions, while BC emissions are basically unchanged.

As the study focuses on impacts from aerosol mitigation, which is subject of air quality control, methane emissions are left unchanged. Having a much longer lifetime than aerosols, methane is almost uniformly mixed in the atmosphere and its warming impact



should be similar to impacts of  $\text{CO}_2$  (e.g. Stohl *et al* 2015). All experiments include a multiyear average of forest and grassland fire emissions from the ACCMIP MACCity biomass burning emission dataset (Lamarque *et al* 2010). Mineral dust and sea spray emissions are calculated online by the atmospheric model in CESM.

### 2.3. Uncertainties

In order to evaluate complex nonlinear interactions, which may not be always detected in ensemble averages, the detection of remote impacts of aerosol emissions on Arctic warming is based on single simulations (section 3). We also analysed ensemble means from four CMIP5 ensembles containing 25 historical simulations forced only by anthropogenic aerosols and made by CCSM4 (Marsh *et al* 2013), CESM/CAM5 (Meehl and Washington 2013) and GISS-E2 (Miller *et al* 2014) models (supplementary table S1). CCSM4 is similar to our model, while CESM/CAM5 and GISS-E2 include aerosol-cloud

interactions. In CMIP5 atmospheric aerosol optical depths (AOD) strongly increase after 1950 over North America, Europe and China (supplementary figure S3).

The uncertainty due to internal decadal variability, that may eventually include naturally strong El Niño events, is addressed by prolonging each simulation until 2065 and fixing anthropogenic emissions and  $\text{CO}_2$  concentrations at the level of year 2050. Since carbon dioxide and pollution emissions in each experiment are approximately constant after 2030, all simulations are forced over more than three decades by practically invariant emissions. An ensemble estimated uncertainties in our model due to small errors in initial states. In BMI, the instantaneous state on 15 January 2035 was substituted with 4 randomly chosen atmospheric states from the same month and the ensemble was integrated for 15 years. Standard deviation of ensemble pentads provides an estimate of uncertainty in all experiments and simulated periods. It is similar to standard deviations estimated over 100 years from 5 CMIP5 ensembles (supplementary

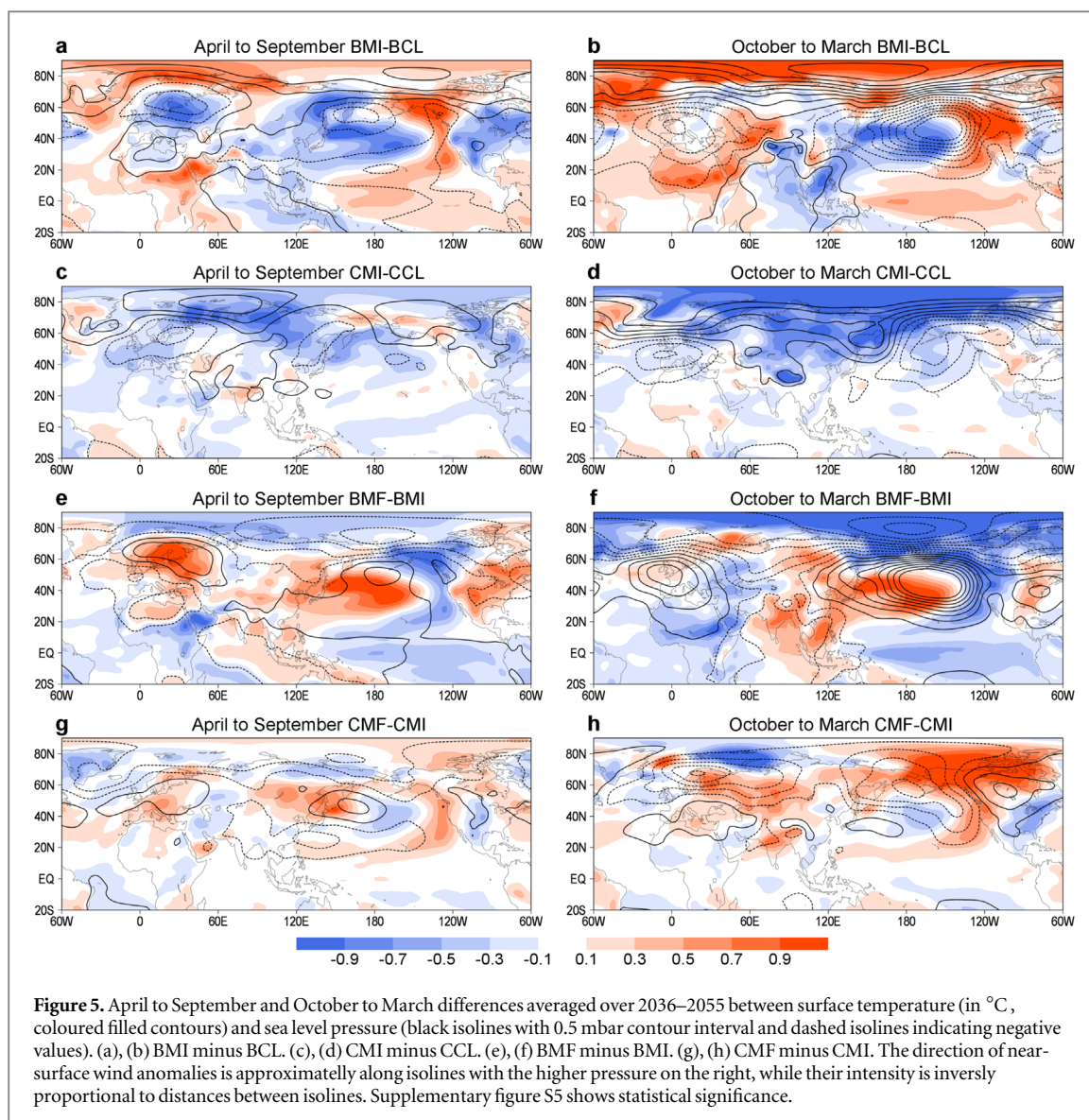


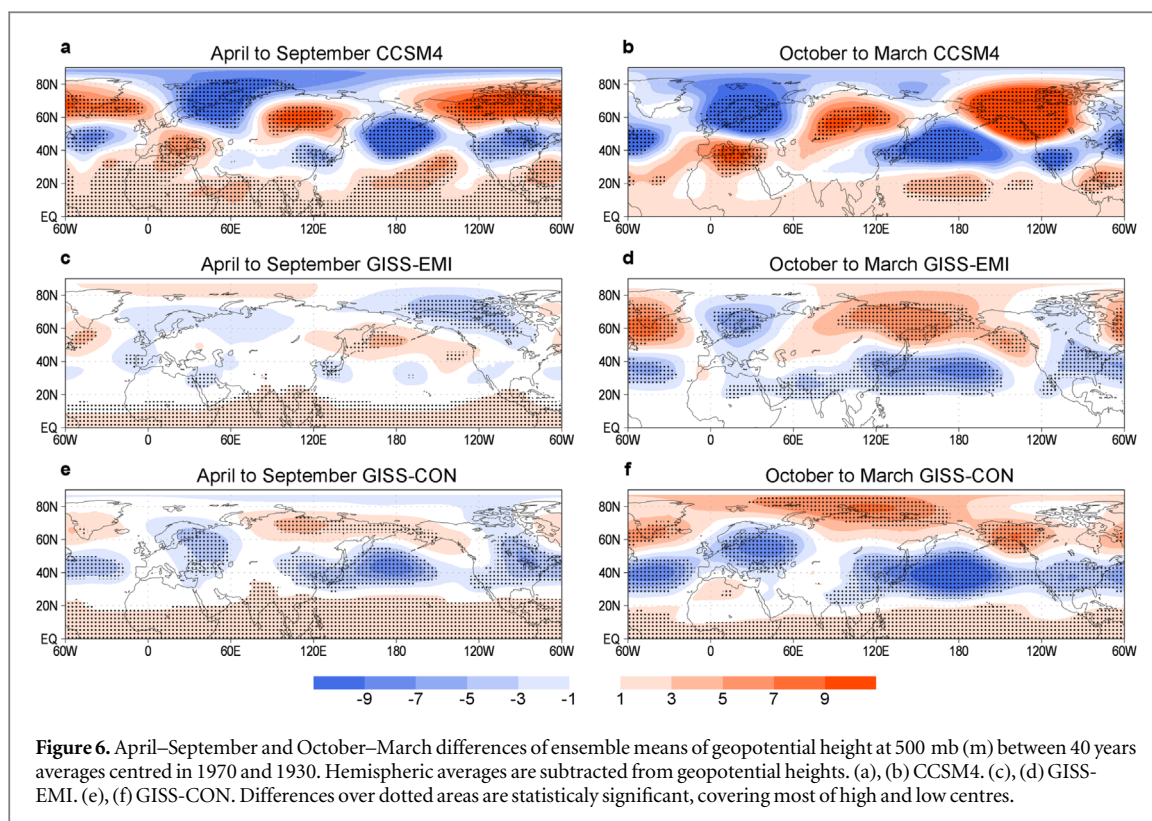
table S2). The statistical significance of model outputs is estimated by the two-sided Student's *t*-test with 95% confidence interval.

### 3. Future atmospheric aerosol forcing of Arctic warming

The Arctic sea-ice cover in September is reduced in all four experiments (figure 2(a)). Differences between experiments are the largest between 2045–2055 showing the greatest loss in BMI with  $1.2 \times 10^6$  km<sup>2</sup> less than in BCL, consistently with the previously estimated increase of Arctic warming and sea-ice loss due to aerosol emission reductions (Westervelt *et al* 2015, Acosta Navarro *et al* 2016, Acosta Navarro *et al* 2017). When the CO<sub>2</sub> concentration is limited in experiment CCL,  $1.2 \times 10^6$  km<sup>2</sup> more sea-ice is preserved than in BCL, which is consistent with reduced global warming due to lower CO<sub>2</sub> concentrations. On the other hand, contrary to previous studies (Westervelt *et al* 2015, Acosta Navarro *et al* 2016, Acosta Navarro *et al* 2017),

reduced aerosol emissions combined with lower CO<sub>2</sub> concentrations in CMI result in the preservation of an additional  $1.3 \times 10^6$  km<sup>2</sup> of sea-ice area.

Zonal averages of near-surface temperatures in 2050 show an impact from high and low CO<sub>2</sub> concentrations, having 0.5 °C lower temperatures in the 'Climate' scenarios almost at every latitude in the Southern and Northern Hemispheres, while lower aerosol emissions do not produce significant impacts (figure 2(b)). In the Arctic there is enhanced warming in all experiments. In agreement with sea-ice cover differences, near the surface BCL is 0.8 °C warmer than CCL, BMI is 1.0 °C warmer than BCL and CCL is 0.7 °C warmer than CMI. Regional differences with opposite signs in sea-ice coverage and near-surface temperatures due to aerosol reductions with high and low CO<sub>2</sub> concentrations may be explained by differences in the heat fluxes over the polar cap from 2036–2055. In addition to direct solar radiation anomalies, total heat in the Arctic varies due to anomalous transport from lower latitudes meridionally



through the atmosphere and ocean and due to variations of heat loss through the top of the atmosphere. Sea-ice cover variations depend on the meridional and surface heat flux anomalies in the ocean. Sea-ice melts from approximately April–September, while from October–March it freezes. Supplementary table S3 shows that during melting the ocean in BMI receives more heat than in BCL due to larger surface fluxes consistent with the warmer atmosphere due to larger meridional atmospheric heat transport. In CCL the ocean receives less heat through the surface than in BCL due to colder atmosphere with less radiation at its top. Larger sea-ice cover in CMI with respect to CCL originates from the colder ocean due to weaker meridional heat transport in the ocean.

Reduced  $\text{CO}_2$  concentrations almost uniformly reduce tropospheric temperatures over the whole globe including the Arctic (figure 3(a)) and SST is lower (here SST represents temperature of the top ocean model layer) over the Arctic Ocean (figure 3(d)). On the other hand, reduced BC and organic carbon concentrations in BMI and CMI appear with reduced tropospheric temperatures in the lower and mid-latitudes of the Northern Hemisphere (figures 3(b), (c)), while the tropospheric temperature response in the Arctic seems to differ in BMI and CMI. In BMI Arctic tropospheric warming is enhanced (figure 3(b)) and SST is higher (figure 3(e)), eventually due to higher meridional heat transport in the atmosphere (supplementary table S3). In CMI Arctic tropospheric temperatures do not change significantly (figure 3(c)), but SST is lower (figure 3(f)), probably due to lower

meridional heat transport in the ocean (supplementary table S3). In BMI and CMI, anthropogenic aerosol concentrations and AODs are reduced over much of the Northern Hemispheric subtropics from Africa to Southeast Asia and northward towards Northeast Asia (figures 4(a)–(d)), although the reduction is smaller in CMI due to already lower BC emissions from less burning of fossil fuels (figure 1). Lower AODs in the Northern Hemisphere reduce zonal tropospheric temperatures in the mid-latitudes (figures 3(b), (c)). In BMI the zonally non-uniform forcing of tropospheric temperatures from lower aerosol concentrations forms cyclonic anomalies of geopotential height spreading between Africa and Northeast Asia. They initiate predominant planetary waves propagating into the Arctic (figures 4(a), (b)). In CMI cyclonic anomalies are weaker, initiating a less intense and statistically insignificant planetary wave that only partly penetrates into the Arctic (figures 4(c), (d)).

Reduced  $\text{SO}_2$  emissions in BMF compared to BMI determine a large reduction in AOD between the Atlantic and Pacific Oceans with the planetary wave limited to the middle and low latitudes and an anticyclone over the Pacific Ocean (figures 4(e), (f)). Very similar AOD reduction and anticyclone over the Pacific Ocean appear in CCL compared to BCL (supplementary figure S6), due to the reduced  $\text{SO}_2$  emissions from using less fossil fuel (Klimont *et al* 2017). The AOD reduction in CMF compared to CMI is smaller, because  $\text{SO}_2$  emissions are partly reduced already in CCL, and the planetary wave is insignificant (figures 4(g), (h)). Different atmospheric waves

corresponding to BC and SO<sub>2</sub> forcings indicate a strong impact of the regional distribution of the tropospheric forcing by atmospheric aerosols in agreement with Wang *et al* (2015).

Surface response to the planetary wave perturbation also differs between simulations with high and low CO<sub>2</sub> concentrations (figure 5). With respect to BCL, in BMI, near-surface winds over Scandinavia, indicated by sea level pressure gradients, increase the transport of warm air from West Siberia into the Arctic Ocean increasing surface heat fluxes into the ocean (supplementary table S3) and warmer tropospheric temperature and SST in the Arctic (figures 3(b) and (e)). With lower CO<sub>2</sub> concentrations, sea level pressure differences between CMI and CCL occur more to the south. The cyclonic circulation anomaly over the Atlantic (figures 5(c), (d)) forms the northerly wind anomaly along the coast of Scandinavia opposing the North Atlantic current that carries heat from the North Atlantic Ocean into the Arctic Ocean in agreement with lower lateral ocean transports of heat (supplementary table S3) and lower SST in the Arctic (figure 3(f)). Compared to BMI and CMI, BMF and CMF either reduce or increase surface temperatures in the Arctic depending on the direction of atmospheric transport anomalies produced by planetary waves (figures 5(e)–(h)).

#### 4. Internal climate variability and nonlinear impacts of small changes in the atmospheric circulation

In section 3 model outputs were compared for the decade surrounding 2050, but due to internal climate variability, aerosol reduction impacts on sea-ice melting differ in other decades (figure 2(a)). After 2050 sea-ice cover anomalies in BMI and CCL are reduced, in BCL and BMF it shrinks to lower values than in BMI, while in CMI and CMF it maintains the largest and most stable sea-ice cover throughout the simulation. When averaged over 35 years (supplementary figures S7 and S8), model outputs show very similar planetary waves in each experiment as in figures 4 and 5. On the other hand, their impacts differ, because small changes in direction and intensity of atmospheric transport at the edges of low and high pressure centres may either increase or decrease Arctic warming. This supports the hypothesis on the nonlinear and complex interaction between the Arctic and other latitudes (Overland *et al* 2016). For example, in BMI and CMI very similar near-surface atmospheric circulation anomalies, characterised by high pressure anomalies over the Arctic and low over the North Atlantic, produce different sea-ice cover anomalies due to small differences in the intensity and form of the flow structure between pressure anomalies (figures 5(a)–(d)). In a fully nonlinear manner the remote response in the Arctic is characterised by distinct solutions initiated by similar forcing

perturbations over Asia and changes in the atmospheric circulation in the Northern Hemisphere.

Uncertainties in sea-ice cover are significant at  $\pm 0.6 \times 10^6 \text{ km}^2$  that is less than the impact of the CO<sub>2</sub> forcing, but it is comparable to impacts from air pollution policies (supplementary table S1). Supplementary table S4 shows that ratio between simulated trends of mean global temperature and Arctic sea-ice cover are similar to observed values (Rosenblum and Eisenman 2017).

#### 5. Historical CMIP5 simulations

Increasing aerosol emissions after 1950 in CMIP5 simulations (supplementary figure S3) also initiate predominant planetary waves that are very similar among model ensembles (figure 6). In all ensembles cyclones formed over East Asia and the Pacific Ocean force anticyclones further to the northeast. Amplitudes are the largest in CCSM4 having the highest horizontal resolution, while in summer wave structures far from the sources may differ in different ensembles. In all ensembles, however, anticyclones penetrate into the Arctic. All ensembles further show increasing sea level pressure between the Mediterranean and Southeast Asia, in agreement with Mitchell and Johns (1997), and planetary wave signatures spreading over East Asia and the Pacific Ocean and penetrating into the Arctic (supplementary figure S9). Partly due to small ensemble sizes, signatures of planetary waves in CCSM4 and CESM1/CAM5 are less significant far from source areas, while they are significant in the two larger GISS-E2 ensembles. Historical Arctic sea-ice cover increases after 1950 in the three models simulating indirect effects, while in CCSM4 it decreases (supplementary table S1). Although eventually uncertain in coarse resolution models (Ma *et al* 2014), modifications of clouds by atmospheric aerosols in the Arctic might also have an important impact on sea-ice melting (Wang *et al* 2018).

#### 6. Conclusions

Depending on the background CO<sub>2</sub> concentration and internal variability of climate, future additional changes in pollution emissions, having a regional radiative forcing effect in Asia, may differently contribute to Arctic warming. They may influence Arctic sea-ice cover by initializing predominant planetary waves that eventually propagate into the Arctic. According to geographical positions of their intrusions into the high latitudes, predominant planetary waves may either increase or diminish heat transport from the mid-latitudes. The impact is nonlinear with distinct solutions depending on whether the changes in heat transport happen in the atmosphere or ocean. Ensembles of CMIP5 simulations further confirm the

formation of predominant planetary waves forced by changing regional aerosol concentrations in Asia and propagating into the Arctic. Our results differ from Westervelt *et al* (2015), Acosta Navarro *et al* (2017) and Wang *et al* (2018) who simulate aerosol effects on clouds, that are absent in our study, and predict increased Arctic warming due to reduced anthropogenic aerosol concentrations. Those studies eventually simulate reduced cloud formation in the Arctic (Wang *et al* 2018), that may be uncertain in low resolution models (Ma *et al* 2014), and do not specifically relate atmospheric aerosol concentrations to CO<sub>2</sub> emissions.

This study confirms that policies reducing future CO<sub>2</sub> concentrations may slow down Arctic sea-ice loss. On the other hand, it suggests that future policies additionally improving air quality may have a less certain warming effect in the Arctic. Further understanding of remote effects on sea-ice will require improved simulations of variations of aerosol concentrations in the Arctic including their local interactions with clouds.

## Acknowledgments

We thank four anonymous reviewers for their constructive and useful comments.

## ORCID iDs

S Dobricic  <https://orcid.org/0000-0003-2897-7748>

## References

- Acosta Navarro J C, Varma V, Riipinen I, Seland Ø, Kirkevåg A, Struthers H, Iversen T, Hansson H-C and Ekman A M L 2016 Amplification of Arctic warming by past air pollution reductions in Europe *Nat. Geosci.* **9** 277–81
- Acosta Navarro J C *et al* 2017 Future response of temperature and precipitation to reduced aerosol emissions as compared with increased greenhouse gas concentrations *J. Clim.* **30** 939–54
- Amann M, Klimont Z and Wagner F 2013 Regional and global emissions of air pollutants: recent trends and future scenarios *Annu. Rev. Environ. Resour.* **38** 31–55
- Årthun M, Eldevik M, Smedsrud L H, Skagseth Ø and Ingvaldsen R B 2012 Quantifying the influence of atlantic heat on barents sea ice variability and retreat *J. Clim.* **25** 4736–43
- Baker L H, Collins W J, Olivie D J L, Cherian R, Hodnebrog Ø, Myhre G and Quaas J 2015 Climate responses to anthropogenic emissions of short-lived climate pollutants *Atmos. Chem. Phys.* **15** 8201–16
- Bollasina M, Ramaswamy V and Ming Y 2011 Anthropogenic aerosols and the weakening of the South Asian summer monsoon *Science* **334** 502–5
- Boucher O *et al* 2013 Clouds and aerosols *Climate Change 2013 The Physical Science Basis. Contribution of Working Group I to the Fifth Assessment Report of the Intergovernmental Panel on Climate Change* ed T F Stocker *et al* (Cambridge: Cambridge University Press) pp 572–657
- Clarke A D and Noone K J 1985 Soot in the Arctic snowpack: a cause for perturbations in radiative transfer *Atmos. Environ.* **19** 2045–53
- Cohen J *et al* 2014 Recent Arctic amplification and extreme mid-latitude weather *Nat. Geosci.* **7** 627–37
- Crippa M, Janssens-Maenhout G, Dentener F, Guizzardi D, Sindelarova K, Muntean M, Van Dingenen R and Granier C 2016 Forty years of improvements in European air quality: regional policy-industry interactions with global impacts *Atmos. Chem. Phys.* **16** 3825–41
- Ding Q, Wallace J M, Battisti D S, Steig E J, Gallant A J E, Kim H-J and Gei L 2014 Tropical forcing of the recent rapid Arctic warming in northeastern Canada and Greenland *Nature* **509** 209–12
- Emmons L K *et al* 2010 Description and evaluation of the model for ozone and related chemical tracers, version 4 (MOZART-4) *Geosci. Model Dev.* **3** 43–67
- Granier C *et al* 2011 Evolution of anthropogenic and biomass burning emissions of air pollutants at global and regional scales during the 1980–2010 period *Clim. Change* **109** 163–90
- Guo L, Turner A J and Highwood E J 2015 Impacts of 20th century aerosol emissions on the South Asian monsoon in the CMIP5 models *Atmos. Chem. Phys.* **15** 6367–78
- Hansen J and Nazarenko L 2004 Soot climate forcing via snow and ice albedos *Proc. Natl Acad. Sci.* **101** 423–8
- Hoesly R M *et al* 2018 Historical (1750–2014) anthropogenic emissions of reactive gases and aerosols from the community emission data system (CEDS) *Geosci. Model Dev.* **11** 369–408
- Holland M M, Bailey D A, Briegleb B P, Light B and Hunke E 2012 Improved sea ice shortwave radiation physics in CCSM4: the impact of melt ponds and aerosols on Arctic sea ice *J. Clim.* **25** 1413–30
- Hoskins B J and Karoly D 1981 The steady linear response of a spherical atmosphere to thermal and orographic forcing *J. Atmos. Sci.* **38** 1179–96
- Hunke E C and Lipscomb W H 2008 CICE: the Los Alamos sea ice model, documentation and software, version 4.0 *Los Alamos Nat. Lab. Tech. Rep.* LA-CC-06-012 p 76
- Hurrell J W *et al* 2013 The community earth system model: a framework for collaborative research *Bull. Am. Meteorol. Soc.* **94** 1339–60
- IEA 2012 *Energy Technology Perspectives 2012—Pathways to a Clean Energy System* (Paris: International Energy Agency, IEA/OECD) ([http://iea.org/publications/freepublications/publication/ETP2012\\_free.pdf](http://iea.org/publications/freepublications/publication/ETP2012_free.pdf))
- Jiang Y, Yang X-Q, Liu X, Yang D, Sun X, Wang M, Ding A, Wang T and Fu C 2017 Anthropogenic aerosol effects on East Asian winter monsoon: the role of black carbon-induced Tibetan Plateau warming *J. Geophys. Res. Atmos.* **122** 5883–902
- Klimont Z, Kupiainen K, Heyes C, Purohit P, Cofala J, Rafaj P, Borken-Kleefeld J and Schöpp W 2017 Global anthropogenic emissions of particulate matter including black carbon *Atmos. Chem. Phys.* **17** 8681–723
- Klimont Z, Smith S and Cofala J 2013 The last decade of global anthropogenic sulfur dioxide: 2000–2011 emissions *Environ. Res. Lett.* **8** 014003
- Lamarque J-F *et al* 2010 Historical (1850–2000) gridded anthropogenic and biomass burning emissions of reactive gases and aerosols: methodology and application *Atmos. Chem. Phys.* **10** 7017–39
- Lewinschal A, Ekman A M L and Körnich H 2013 The role of precipitation in aerosol-induced changes in northern hemisphere wintertime stationary waves *Clim. Dyn.* **41** 647–61
- Li Z *et al* 2016 Aerosol and monsoon climate interactions over Asia *Rev. Geophys.* **54** 866–929
- Ma P-L, Rasch P J, Fast J D, Easter R C, Gustafson W I Jr, Liu X, Ghan S J and Singh B 2014 Assessing the CAM5 physics suite in the WRF-Chem model: implementation, resolution sensitivity, and a first evaluation for a regional case study *Geosci. Model Dev.* **7** 755–78
- Marsh D R, Mills M J, Kinnison D E, Lamarque J-F, Calvo N and Polvani L M 2013 Climate change from 1850 to 2005 simulated in CESM1 (WACCM) *J. Clim.* **26** 7372–91
- Meehl G A and Washington W M 2013 Climate change projections in CESM1(CAM5) compared to CCSM4 *J. Clim.* **26** 6287–308

- Menon S, Hansen J, Nazarenko L and Luo Y 2002 Climate effects of black carbon aerosols in China and India *Science* **297** 2250–3
- Miller R L *et al* 2014 CMIP5 historical simulations (1850–2012) with GISS ModelE2 *J. Adv. Model. Earth Syst.* **6** 441–77
- Mitchell J F B and Johns T C 1997 On modification of global warming by sulfate aerosols *J. Clim.* **10** 245–67
- Morgenstern O *et al* 2017 Review of the global models used within phase 1 of the chemistry–climate model initiative (CCMI) *Geosci. Model Dev.* **10** 639–71
- Najafi M R, Zwiers F W and Gillett N P 2015 Attribution of Arctic temperature change to greenhouse-gas and aerosol influences *Nat. Clim. Change* **5** 246–9
- Neale R B 2010 Description of the NCAR community atmosphere model (CAM 4.0) *NCAR Tech. Note* NCAR/TN-XXX + STR p 206
- Oleson K W 2010 Technical description of version 4.0 of the community land model (CLM) *NCAR Tech. Note* NCAR/TN-478 + STR NCAR/TN-478 + STR p 257
- Overland J E, Dethloff K, Francis J A, Hall R J, Hanna E, Kim S-J, Screen J A, Shepherd T G and Vihma T 2016 Nonlinear response of mid-latitude weather to the changing Arctic *Nat. Clim. Change* **6** 992–9
- Peings Y and Magnusdottir G 2014 Forcing of the wintertime atmospheric circulation by the multidecadal fluctuations of the North Atlantic ocean *Environ. Res. Lett.* **9** 034018
- Perlwitz J, Hoerling M and Dole R 2015 Arctic tropospheric warming: causes and linkages to lower latitudes *J. Clim.* **28** 2154–67
- Pithan F and Mauritsen T 2014 Arctic amplification dominated by temperature feedbacks in contemporary climate models *Nat. Geosci.* **7** 2–5
- Ramanathan V, Chung C, Kim D, Bettge T, Buja L, Kiehl J T, Washington W M, Fu Q, Sikka D R and Wild M 2005 Atmospheric brown clouds: impacts on South Asian climate and hydrological cycle *Proc. Natl Acad. Sci. USA* **102** 5326–33
- Rao S *et al* 2017 Future air pollution in the shared socio-economic pathways *Glob. Environ. Change* **42** 346–58
- Rosenblum E and Eisenman I 2017 Sea ice trends in climate models only accurate in runs with biased global warming *J. Clim.* **30** 6265–78
- Serreze M C and Francis J A 2006 The arctic amplification debate *Clim. Change* **76** 241–64
- Shindell D *et al* 2012 Simultaneously mitigating near-term climate change and improving human health and food security *Science* **335** 183–9
- Smith R 2010 The parallel ocean program (POP) reference manual: ocean component of the community climate system model (CCSM) and community earth system model (CESM) *Los Alamos Nat. Lab. Tech. Rep.* LAUR-10-01853 p 141
- Smith S J, Van Aardenne J, Klimont Z, Andres R J, Volke A and Arias S D 2011 Physics anthropogenic sulfur dioxide emissions: 1850–2005 *Atmos. Chem. Phys.* **11** 1101–16
- Stohl A *et al* 2015 Evaluating the climate and air quality impacts of short-lived pollutants *Atmos. Chem. Phys.* **15** 10529–66
- Swart N C, Fyfe J C, Hawkins E, Kay J E and Jahn A 2015 Influence of internal variability on Arctic sea-ice trends *Nat. Clim. Change* **5** 86–9
- Takahashi C and Watanabe M 2016 Pacific trade winds accelerated by aerosol forcing over the past two decades *Nat. Clim. Change* **6** 768–72
- UNEP/WMO 2011 *Integrated Assessment of Black Carbon and Tropospheric Ozone* (Nairobi: United Nations Environment Programme and World Meteorological Organization)
- Wang Y, Jiang J and Su H 2015 Atmospheric responses to the redistribution of anthropogenic aerosols *J. Geophys. Res. Atmos.* **120** 9625–41
- Wang Y, Jiang J H, Su H, Choi Y-S, Huang L, Guo J and Yung Y L 2018 Elucidating the role of anthropogenic aerosols in arctic sea ice variations *J. Clim.* **31** 99–114
- Wang Y, Zhang R and Saravanan R 2014 Asian pollution climatically modulates mid-latitude cyclones following hierarchical modelling and observational analysis *Nat. Commun.* **5** 3098
- Westervelt D M, Horowitz L W, Naik V, Golaz J C and Mauzerall D L 2015 Radiative forcing and climate response to projected 21st century aerosol decreases *Atmos. Chem. Phys.* **15** 12681–703
- Yang Q, Bitz C M and Doherty S J 2014 Offsetting effects of aerosols on Arctic and global climate in the late 20th century *Atmos. Chem. Phys.* **14** 3969–75